

## Supplementary Information

### pH-triggered formation of nanoribbons from yeast-derived glycolipid biosurfactants

Anne-Sophie Cuvier, Jan Berton, Christian V. Stevens, Giulia C. Fadda, Florence Babonneau, Inge N. A. Van Bogaert, Wim Soetaert, Gérard Pehau-Arnaudet, Niki Baccile\*

#### Sections

<b>S.1</b> - <i>Complementary experimental section</i>	P.S2
<b>S.2</b> - <i>Solution NMR of acidic C18:1-cis and C18:0 sophorolipids</i>	P.S3
<b>S.3</b> - <i>HPLC of acidic C18:1-cis and C18:0 sophorolipids</i>	P.S4
<b>S.4</b> - <i>Characterization techniques</i>	P.S5
<b>S.5</b> - <i>Detailed analysis of the pH-titration curve</i>	P.S9
<b>S.6</b> - <i>Additional cryo-TEM data on the chiral supramolecular structures</i>	P.S10
<b>S.7</b> - <i>Demonstration of the presence of twisted using sample-holder tilting in cryo-TEM</i>	P.S11
<b>S.8</b> - <i>WAXS experiments</i>	P.S12
<b>S.9</b> - <i>Solid state NMR spectroscopy</i>	P.S13

## S.1 Complementary experimental section.

*Synthesis of acidic C18:1-cis sophorolipid:* A sophorolipid mixture containing several natural types of sophorolipids (lactonic versus acidic, different degree of acetylation) was obtained by fed-batch cultivation of *Starmerella (Candida) bombicola* ATCC 22214 in a five liter vessel from Braun-Biostat®. A temperature of 30°C, a pH of 3.5 (adjusted by adding NaOH), an airflow rate of 1 vvm and a stirring rate of 650 rpm was applied and controlled by the Biostat® B control unit. A pre-culture of 0.2 L was inoculated to the 4 L fermentation medium described by Lang et al.<sup>1</sup> Additional glucose and rapeseed oil were added in a fed-batch way. The culture was harvested after 10 days and crude sophorolipids were recovered from the broth after precipitation by heating at 60 °C. The sophorolipids, mainly occurring in the lactonic form, were crystallized in distilled water: 500 mL water was added to 100 g crude sophorolipids and the mixture was shaken overnight at 200 rpm and 4°C. White crystals were collected after centrifugation for 5 min at 5600 g and washed three times with ice-cold distilled water to remove residual yellowish medium contaminants. The crystallized sophorolipids were converted to acidic unacetylated sophorolipids by alkaline hydrolysis.<sup>2</sup> The solution was brought to pH= 4.0 and acidic sophorolipids were extracted twice with one volume of technical ethanol/ethylacetate (1/1). After vacuum evaporation of the solvent, the sophorolipid crystals were re-suspended in water and freeze-dried. The fatty acid moiety of the obtained sophorolipid mainly consisted of oleic acid (C18:1-cis).

*Synthesis of the acidic C18:0 sophorolipid:* 1.47 g (2.36 mmol) C18:1-cis sophorolipid was dissolved in 100 mL MeOH under a N<sub>2</sub> atmosphere. 0.147 mg (10 w/w%) Pd/C (10%) was added in portions. The reaction mixture was stirred for 7 hours under 5 bar H<sub>2</sub> atmosphere, after which it was filtered over celite. After removal of the solvent *in vacuo* a white solid was obtained which was finally lyophilized overnight to give 1.11 g (1.78 mmol) of the saturated acidic C18:0 sophorolipid.

---

<sup>1</sup> S. Lang, A. Brakemeier, R. Heckmann, S. Spöckner, U. Rau, *Chim. Oggi* **2000**, *10*, 76–79

<sup>2</sup> U. Rau, R. Heckmann, V. Wray, S. Lang, T. U. Braunschweig, *Biotechnol. Lett.* **1999**, *21*, 973–977

## S.2 Solution NMR of acidic C18:1-cis and C18:0 sophorolipids

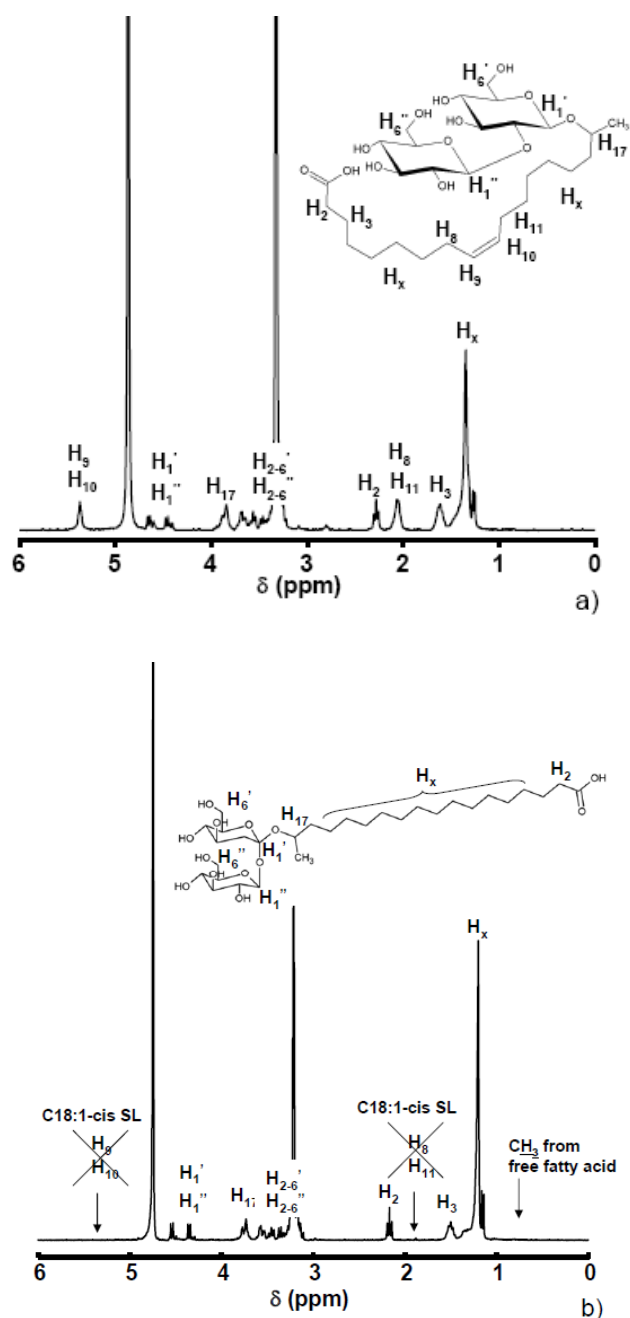


Figure S1 –  $^1\text{H}$  NMR spectra of acidic sophorolipids (a) C18 :1-*cis* and (b) C18-0

### Spectral data C18:1-*cis* sophorolipid

$^1\text{H}$  NMR (300 MHz,  $\text{CD}_3\text{OD}$ )  $\delta$ : 1.15 (3H, d,  $J = 6.1$  Hz,  $\text{CH}_3$ ), 1.18 - 1.42 (20H, br. s, aliphatic chain), 1.42 - 1.58 (3H, m, aliphatic chain), 1.88 - 2.01 (4H, m,  $\text{CH}_2\text{CHCHCH}_2$ ), 2.16 (2H, t,  $J = 7.4$  Hz,  $\text{CH}_2\text{COOH}$ ), 3.11 - 3.78 (13H, m, 9 x  $\text{CHOH}$  + 4 x  $\text{CH}_2\text{OH}$ ), 4.35 (1H, d,  $J = 7.7$  Hz,  $\text{CHO}_2$ ), 4.54 (1H, d,  $J = 7.7$  Hz,  $\text{CHO}_2$ ), 5.17 - 5.32 (2H, m,  $\text{CHCH}$ ).

### Spectral data C18:0 sophorolipid

$^1\text{H}$  NMR (300 MHz,  $\text{CD}_3\text{OD}$ )  $\delta$ : 1.15 (3H, d,  $J = 6.1$  Hz,  $\text{CH}_3$ ), 1.17 - 1.40 (25H, br. s, aliphatic chain), 1.45 - 1.55 (3H, m, aliphatic chain), 2.17 (2H, t,  $J = 7.2$  Hz,  $\text{CH}_2\text{COOH}$ ), 3.10 - 3.78 (13H, m, 9 x  $\text{CHOH}$  + 4 x  $\text{CH}_2\text{OH}$ ), 4.35 (1H, d,  $J = 7.7$  Hz,  $\text{CHO}_2$ ), 4.54 (1H, d,  $J = 7.7$  Hz,  $\text{CHO}_2$ )

### S.3 HPLC of of acidic C18:1-*cis* and C18:0 sophorolipids

HPLC analysis<sup>3</sup> of the sophorolipids before and after the hydrogenation process confirms the conversion of the C18:1-*cis* sophorolipids into the completely saturated C18:0 sophorolipid. HPLC also shows that the level of hydrophobic impurities is below the detection limit of the instrument.

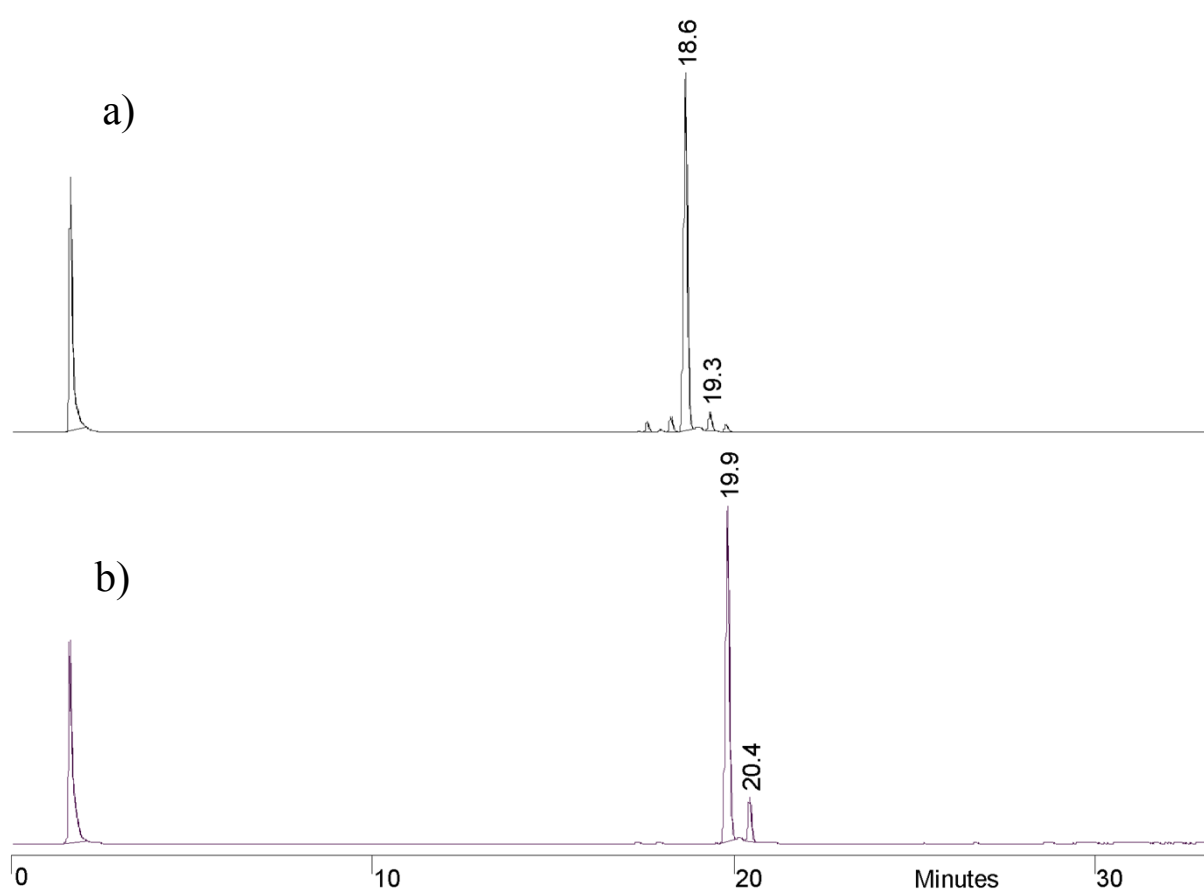


**Figure S2: (A) Acidic C18:1-*cis* sophorolipids. The peak at 18.6 minutes originates from the acidic, non-acetylated sophorolipid with a 17-hydroxy-*cis*-octadecenoic acid moiety. The 18-hydroxy form elutes at 19.3 minutes. (B) Acidic C18:0 sophorolipids, containing 17- and 18-hydroxy- octadecanoic acid, elute at 19.9 and 20.4 minutes respectively.**

<sup>3</sup> Van Bogaert, I.N.A., Sabirova, J., Develter, D., Soetaert, W. & Vandamme, E.J. Knocking out the MFE-2 gene of *Candida bombicola* leads to improved medium-chain sophorolipid production. *FEMS Yeast Research*, 2009, 9, 610–617

#### **S.4 Characterization techniques**

*Transmission electron microscopy* (TEM) experiments under cryogenic conditions were performed on a FEI Tecnai 120 Twin microscope operating on 120 kV equipped with a high resolution Gatan Orius CCD numeric camera. The sample holder was a Gatan Cryoholder (Gatan 626DH, Gatan). Additional experiments have been done on a Tecnai F20 at the PFMU, Institut Pasteur (Paris, France). The microscope operates at 200 kV and magnification was 80.000 fold. A Gatan ultrascan 4000 camera was used to acquire the image. On both microscopes, DigitalMicrograph™ software was used for image acquisition. Cryofixation was either done on a EMGP, Leica (Austria) instrument or on a home made cryo-fixation device. The solutions were deposited on holey carbon coated TEM copper grids (10  $\mu\text{m}$ , Quantifoil R2/2, Germany). Excess solution was removed and the grid was immediately plunged into liquid ethane. All grids were kept at liquid nitrogen during storage and at 180°C throughout all experimentation. All grids were stored under liquid nitrogen until used for image acquisition.

*Field emission scanning electron microscopy* (FE-SEM) experiments were carried out on a Hitachi SU70 (FE-SEM) microscope. Samples were previously freeze-dried in an Avanteq Alpha 2-4 LO freeze drying machine. The resulting powders were deposited on a carbon film and coated with 5 nm platinum.

*Dynamic light scattering* (DLS) measurements were run on a Malvern Zetasizer Nano ZS instrument ( $\lambda = 633\text{nm}$ ) at constant shutter opening and same sample-to-detector distance. The diffused light is expressed in terms of the derived count rate (DCR) in kilocounts-per-seconds (kcps).

*pH titration* was done on a solution containing C18:0 sophorolipids at  $\text{pH} < 3$  with  $\mu\text{molar}$  amounts ( $\sim 5 \mu\text{L}$ ) 0.1 M solution of NaOH. The compound is initially solubilized at  $\text{pH} = 11$  using  $\mu\text{molar}$  amounts of a 5 M NaOH solution; the pH is then lowered with an equivalent amount of 5 M HCl to  $\text{pH} < 3$ , at which titration starts.

*Small Angle Neutron Scattering* (SANS) was performed at the Léon Brillouin Laboratory (LLB, Orphée Reactor, Gif-sur-Yvette, France) on the PACE beamline. The spectrometer configuration was adjusted to cover two different q-ranges. The small angle region  $6.90 \times 10^{-3} \text{ \AA}^{-1} < q < 7.30 \times 10^{-2} \text{ \AA}^{-1}$  is obtained with a neutron wavelength,  $\lambda$ , of 6  $\text{ \AA}$  and a sample-to-detector distance, D, of 4.7 m. The medium angle region covers a q-range  $2.90 \times 10^{-2} \text{ \AA}^{-1} < q < 3.00 \times 10^{-1} \text{ \AA}^{-1}$  at  $\lambda = 6 \text{ \AA}$  with  $D = 1.0 \text{ m}$ . q is defined as  $(4\pi/\lambda)\sin\theta/2$ , where  $\theta$  is the scattering angle between the incident and the scattered neutron beams. All samples are introduced in a 2

mm quartz cell and studied at  $T = 22^\circ\text{C}$ . Data treatment is done with the PAsiNET.MAT software package provided at the beamline and available free of charge. Absolute values of the scattering intensity are obtained from the direct determination of the number of neutrons in the incident beam and the detector cell solid angle. The 2D raw data were corrected for the ambient background and empty cell scattering and normalized to yield an absolute scale (cross section per unit volume) by the neutron flux on the samples. The data were then circularly averaged to yield the 1-D intensity distribution,  $I(q)$ . Incoherent signal was substrated by measuring the background value at high- $q$ .

#### *Fit of SANS data*

Data have been fitted using the software SANSview©, available free of charge at <http://danse.chem.utk.edu/sansview.html>.

The form factor of chiral ribbons has a  $I(q) \sim q^{-2}$  dependence, which is equivalent to the form factor of a flat sheet. If the former is not implemented in the SANSview software package, the latter can be easily used instead, at least in a qualitative way.<sup>4</sup> At the same time, we also used a simple, model-independent, function which contains a two-power dependence. The fitting parameters for each of the fits are the following: 1) *lamellar form factor*: background = 0.0003  $\text{cm}^{-1}$ ;  $bi\_thick = 128 \text{ \AA}$ ; scale = 0.0033;  $sld\_bi = 2 \times 10^{-6} \text{ \AA}^{-2}$ ;  $sld\_sol = 6.36 \times 10^{-6} \text{ \AA}^{-2}$ ; distribution of  $bi\_thick = PD(\text{ratio}) = 0.3$  (gaussian), where  $Bi\_thick$  is the bilayer thickness;  $sld$  is the scattering length density of bilayer ( $sld\_bi$ ) or solvent ( $sld\_solv$ );  $PD$  is the polydispersity of the bilayer;  $coef\_A$  is a scaling coefficient. 2) *Two-power law function*: background = 0.0003  $\text{cm}^{-1}$ ;  $coef\_A = 0.0035$ ;  $qc = 0.0185 \text{ \AA}^{-1}$ ;  $power2 = 4$ ;  $power1 = 2$ , where  $power1$  and  $power2$  are the values of the exponentials used in the function,  $qc$  is the inflection point between the two power laws. For more information on the type of function, please refer to <http://danse.chem.utk.edu/downloads/ModelfuncDocs.pdf>

*2D  $^1\text{H}$ - $^1\text{H}$  Back-to-Back (BABA) Magic Angle Spinning (MAS) NMR experiments* were recorded on a Bruker Avance 700 MHz (16.4 T) spectrometer using a fast-MAS probe (1.3 mm) to increase resolution in the proton spectrum ( $\nu_{\text{MAS}} = 65 \text{ kHz}$ ). The freeze-dried sample was spun at room temperature and the  $^1\text{H}$  signal was filtered using a single-quantum double-quantum homonuclear excitation-reconversion pulse sequence (Back-to-Back, BABA).<sup>5</sup> Direct proximities ( $< 5 \text{ \AA}$ ) between through-space dipolar coupled protons are explored using one single loop, the lowest number of loops corresponding to the closest protons. 128  $t_1$

---

<sup>4</sup> Hamley, I. W. *Macromolecules* **2008**, *41*, 8948

<sup>5</sup> M. Feike, D. E. Demco, R. Graf, J. Gottwald, S. Hafner, H. W. Spiess, *J. Magn. Res., Series A* **1996**, *122*, 214–221

increments with 32 transients each were recorded and quadrature detection in the indirect dimension was realized using the States method.

The BABA pulse sequence provides an exploitable signal on the diagonal of the 2D spectrum, as it discriminates between coupled and non-coupled protons: if on-diagonal cross-peaks are observed, the corresponding protons are dipolarly coupled and, hence, close in space.

*2D  $^{13}\text{C}$ - $^1\text{H}$  solid-state HETeronuclear CORrelation (HETCOR) Magic Angle Spinning (MAS) Frequency-Switched Lee-Goldberg (FSLG) NMR experiments* have been acquired on a Bruker Avance 300 MHz (7 T) spectrometer using 4 mm CRAMPS zirconia rotor spinning at a MAS frequency of  $\nu_{\text{MAS}} = 12.5$  kHz.  $^1\text{H}$  chemical shifts were referenced relative to tetramethylsilane (TMS;  $\delta = 0$  ppm). For this experiment, the sample was previously concentrated into a wet gel by centrifugation, which was directly located in the middle of the CRAMPS rotor. The temperature in the probe was then set to  $T = 263$  K throughout the experiment. This was done using the integrated BCU-X temperature controller unit. The HETCOR experiment was recorded using a 2D version of a standard CP pulse sequence provided in the TOPSPIN 3.1 Bruker software package (HXHETCOR). The cross-polarization time was set to 3 ms while the recycling time was 2 s. 36  $t_1$  increments with 5600 transients each were recorded and quadrature detection in the indirect dimension was realized using the States method. To recover high-resolution in the indirect  $^1\text{H}$  dimension, it was crucial to use a Frequency-Switched Lee-Goldberg (FSLG) homonuclear decoupling method,<sup>6</sup> directly implemented in the pulse sequence. The optimum LG radio-frequency field was found to be 75000 Hz and the LG decoupling power equal to 100 W. The offset in the indirect dimension ( $^1\text{H}$ ) was set out of the region of interest (0-6 ppm) in order to avoid artefacts overlapping the signal. The chemical shift in the indirect dimension was calibrated and rescaled with respect to the  $^1\text{H}$  signal recorded on the same sample at high MAS ( $\nu_{\text{MAS}} = 65$  kHz) and for which no homonuclear high-power decoupling was applied.

*2D  $^{13}\text{C}$ - $^1\text{H}$  solid-state HETeronuclear CORrelation (HETCOR) Magic Angle Spinning (MAS) NMR experiments with homonuclear DUMBO decoupling* have been acquired on a Bruker Avance 700 MHz (16.4 T) spectrometer using 2.5 mm zirconia rotor spinning at a MAS frequency of  $\nu_{\text{MAS}} = 20$  kHz.  $^1\text{H}$  chemical shifts were referenced relative to tetramethylsilane (TMS;  $\delta = 0$  ppm). For this experiment, the sample was previously concentrated into a wet gel

---

<sup>6</sup> B.-J. van Rossum, H. Förster, H.J.M. de Groot, J. Magn. Res., 1997, 124, 516

by centrifugation and let dry under air at room. all experiments were recorded at room temperature. The HETCOR experiment was recorded using a 2D version of a standard CP pulse sequence provided in the TOPSPIN 3.1 Bruker software package (HXHETCOR). The cross-polarization time was set to 3 ms while the recycling time was 2 s. 62  $t_1$  increments with 800 transients each were recorded and quadrature detection in the indirect dimension was realized using the States method. To recover high-resolution in the indirect  $^1\text{H}$  dimension, it was crucial to use a DUMBO homonuclear decoupling method,<sup>7</sup> directly implemented in the pulse sequence. The optimum decoupling radio-frequency field was found to be 104 kHz and the decoupling power equal to 70 W. The optimum  $^1\text{H}$  offset to reduce artifacts was found to be 16403 Hz while the DUMBO decoupling interval was optimized to 24  $\mu\text{s}$ . Despite all our efforts, we were not able to completely eliminate the zero-frequency peak<sup>8</sup> in the indirect dimension ( $^1\text{H}$ ) which slightly perturbs the relative intensities at  $\delta_{1\text{H}} = 1.3$  ppm in the corresponding 2D HETCOR map. The chemical shift in the indirect dimension was calibrated and rescaled with respect to the  $^1\text{H}$  signal recorded on the same sample at high MAS ( $\nu_{\text{MAS}} = 65$  kHz) and for which no homonuclear high-power decoupling was applied.

*Circular Dichroism* (CD) has been recorded on a Jasco J-810 spectropolarimeter between 190 nm and 300 nm with a 0.1 nm step for solutions at a concentration of 5 mg/mL. C18:0 sphorolipids were dissolved at pH= 11 in deionized water and pH was successively decreased with 0.05 M and 0.025 M HCl solutions and then loaded into a 1 mm quartz cuvette for measurements.

---

<sup>7</sup> D. Sakellariou, A. Lesage, P. Hodgkinson, L. Emsley, Homonuclear dipolar decoupling in solid-state NMR using continuous phase modulation, *Chem. Phys. Lett.*, 2000, 319, 253–260

<sup>8</sup> a) R. Siegel, L. Mafra, J. Rocha Improving the  $^1\text{H}$  indirect dimension resolution of 2D CRAMPS NMR spectra: A simulation and experimental investigation, *Sol. St. Nucl. Magnet. Res.*, 2011, 39, 81–87 ; b) A. Lesage, D. Sakellariou, S. Hediger, B. El $\square$ ena, P. Charmont, S. Steuernagel, L. Emsley Experimental aspects of proton NMR spectroscopy in solids using phase-modulated homonuclear dipolar decoupling, *J. Magn. Res.*, 2003, 163, 105–113



### S.5 Detailed analysis of the pH-titration curve shown in Figure 3 of the main text

For the sake of the discussion below only, we define, SL-COOH being the acronym for the C18:0 sphorolipid, SL-COOH<sub>solid</sub> referring to its solid fraction and SL-COOH<sub>solu</sub> to its soluble fraction.

At pH 2.12, the following species coexist in water: SL-COOH<sub>solid</sub>, SL-COOH<sub>solu</sub>, HCl and NaCl. The following equilibria exist at acidic pH:



where, HCl is the excess of strong acid and NaCl is the salt, H<sup>+</sup><sub>sa</sub> is the protic contribution from the dissociation of the strong acid (HCl), H<sup>+</sup><sub>wa</sub> is the protic contribution of the weak acid (SL-COOH<sub>solu</sub>). The equivalent point N°1 in Figure 3 (main text) corresponds to the titration of H<sup>+</sup><sub>sa</sub>, for which an equivalent volume V<sub>eq1</sub> = 94 μL is found. The pH at the equivalence is pH(V<sub>eq1</sub>) = 5.2, which then depends on the soluble fraction of C18:0 sphorolipid (Eq.S2). At pH(V<sub>eq1</sub>) = 5.2, it is also possible to estimate SL-COOH<sub>solu</sub>. Since [SL-COOH<sub>solid</sub> + SL-COOH<sub>solu</sub>] = N<sub>C18:0</sub> is the total molar amount of C18:0 sphorolipid equal to the initial concentration, it is eventually possible to quantify SL-COOH<sub>solid</sub>.

The concentration of SL-COOH<sub>solu</sub> is calculated using the following equation (Eq.S3):

$$\text{pH}(V_{\text{eq1}}) = \frac{1}{2} (\text{pK}_{\text{SLC18:0}} - \log C_{\text{COOHsolu}}) \quad \text{Eq.S3}$$

where pK<sub>SLC18:0</sub> is the pK value for C18:0 sphorolipid, which in first approximation is assumed to be equal to 4.8, the pKa of stearic acid; C<sub>COOHsolu</sub> is the concentration of SL-COOH<sub>solu</sub> at V<sub>eq1</sub>. Solving Eq.S3 gives C<sub>COOHsolu</sub> = 10<sup>-6</sup> M, which, if compared to the initial concentration of C18:0 sphorolipid, 1.6·10<sup>-3</sup> M, it is obviously negligible. At acidic pH the process of assembling is practically quantitative. This can be verified further. The second equivalence at pH = 8.4 and V<sub>eq2</sub> = 140 μL (N° 2 on Figure 3 in the main text) is also quite interesting as it corresponds to the titration of the SL-COOH<sub>solid</sub>. The difference ΔV<sub>eq</sub> = V<sub>eq2</sub> - V<sub>eq1</sub> is 46 μL, which corresponds to an OH<sup>-</sup> concentration of ~ 2.3·10<sup>-3</sup> M. Very interestingly, this amount is consistent with the initial concentration of C18:0 sphorolipid in solution, 1.6·10<sup>-3</sup> M. Thus, at pH = 8.5 practically the entire amount of C18:0 sphorolipid is titrated and dissolved in solution.

## S.6 Additional cryo-TEM data on the chiral supramolecular structures

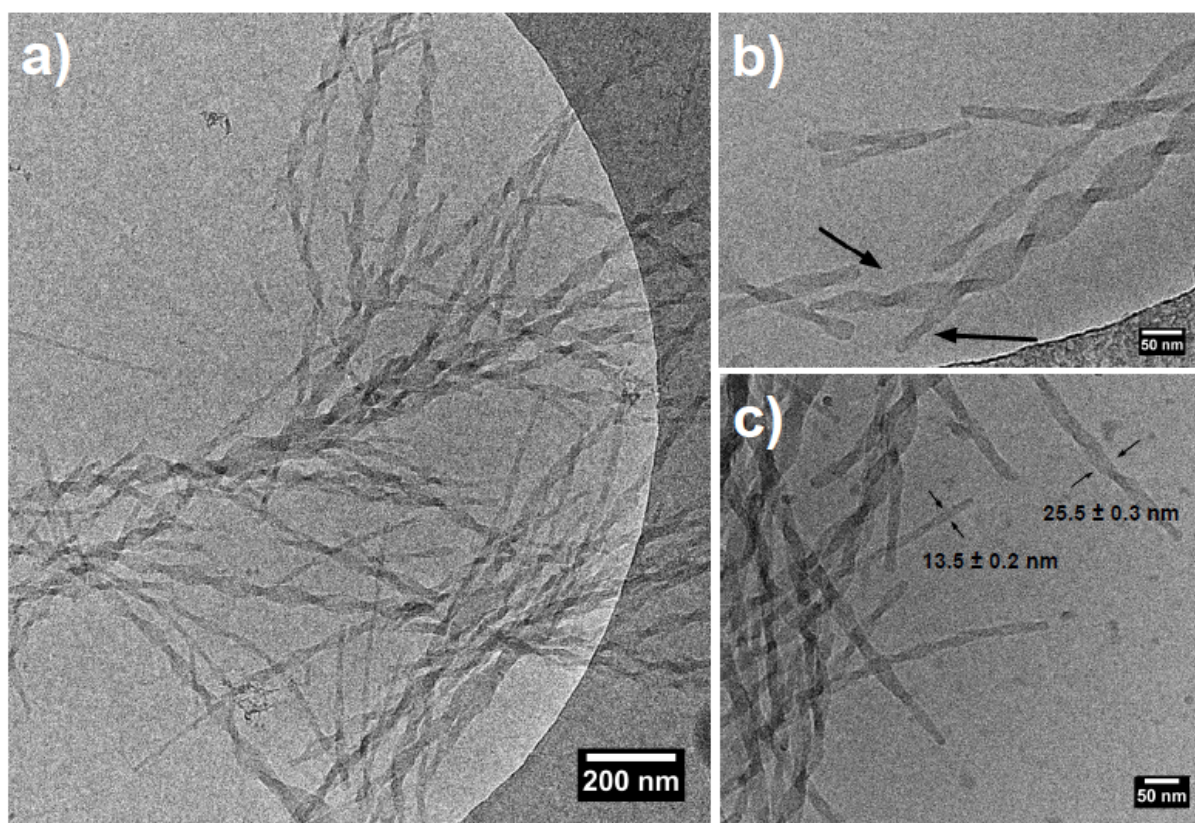


Figure S3 - Cryo-TEM images of self-assembled C18:0 sophorolipid structures ( $c= 5\text{mg/mL}$ ,  $\text{pH}= 6$ )

### S.7 Demonstration of the presence of twisted ribbons using sample-holder tilting in cryo-TEM

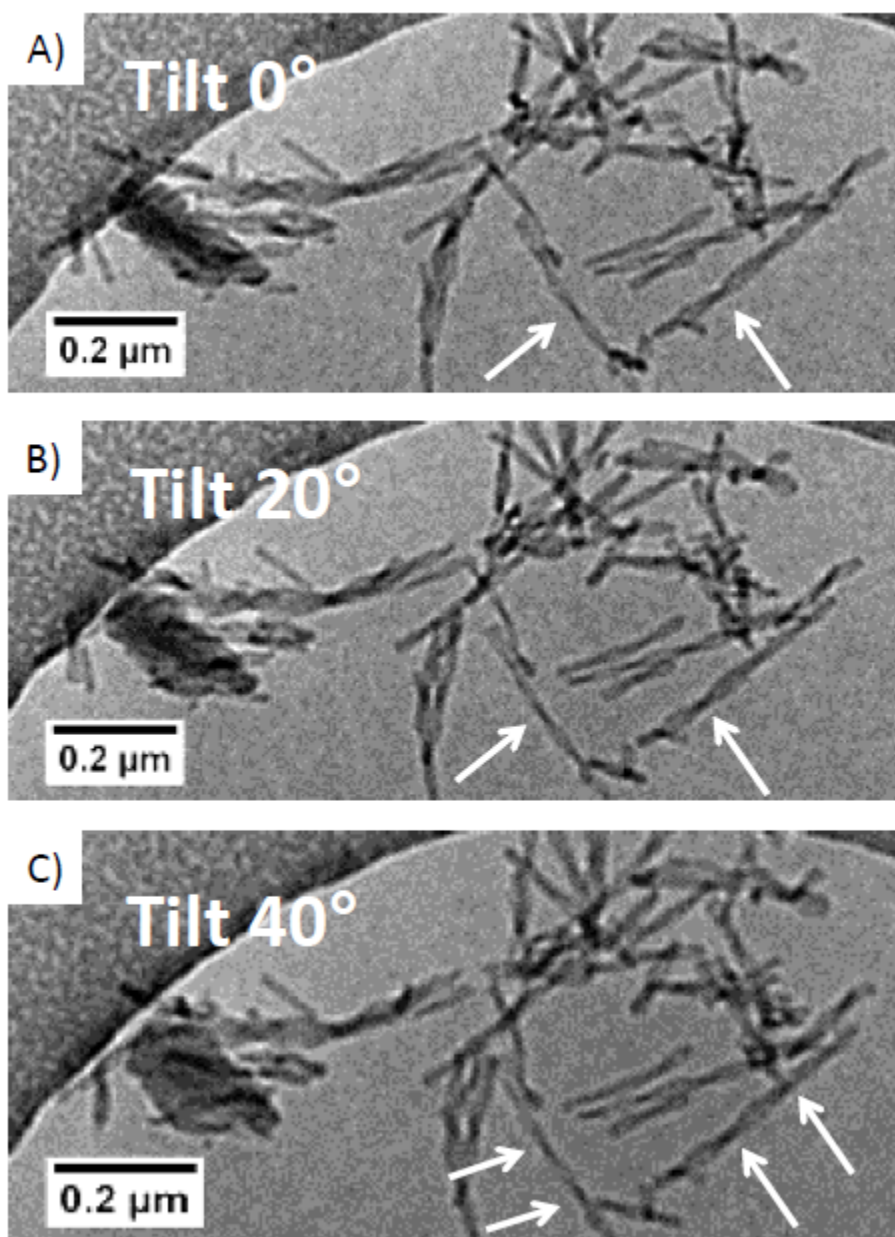


Figure S4 - Tilted cryo-TEM images of the self-assembled C18:0 sophorolipid structures at  $c = 2\text{mg/mL}$ ,  $\text{pH} = 2$ . Tilts angles are (A)  $0^\circ$ ; (B)  $+20^\circ$ ; (C)  $+40^\circ$ .

Picture C in Figure S4 is tilted by an angle of  $40^\circ$  from image A. One can see how the helix's position is modified, thus distinguishing two knots appearing in C while there is only one in A.

## S.8 WAXS experiments

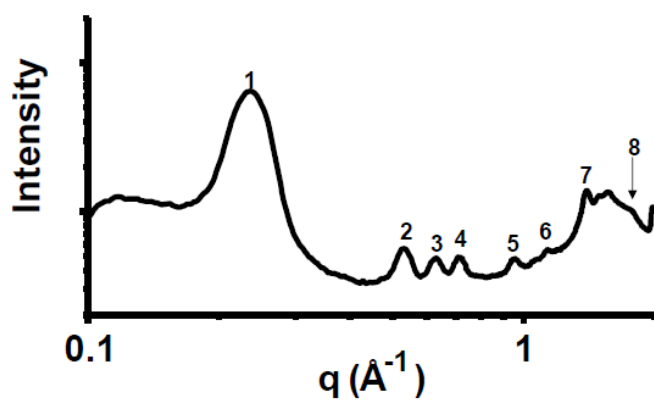


Figure S5: WAXS data for the freeze-dried C18:0 sophorolipid samples obtained at pH= 6. The d-values attributed to each peak are given in Table S1

Table S1 – Peak positions and corresponding d-values obtained from WAXS data on C18:0 sophorolipids at pH= 6

Peak No.	pH= 6	
	q (Å <sup>-1</sup> )	d (nm)
1	0.24	2.65
2	0.53	1.19
3	0.63	1.00
4	0.71	0.88
5	0.96	0.66
6	1.14	0.55
7	1.40	0.45
8	1.75	0.36

## S.9 Solid state NMR spectroscopy

This section has the goal of using solid state NMR spectroscopy to confirm the adoption of a symmetrical MLM configuration by the C18:0 sophorolipid molecules inside the ribbons.

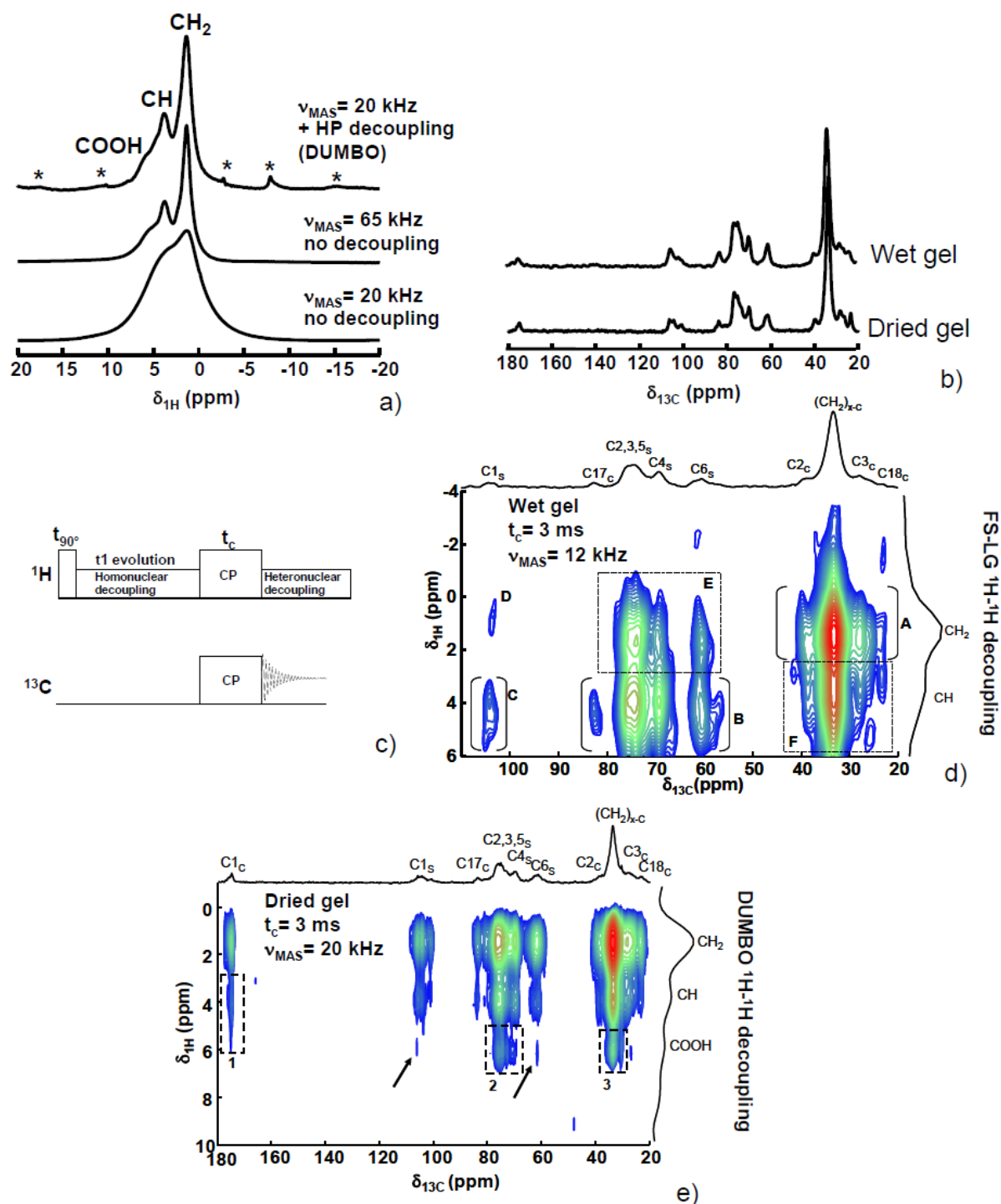


Figure S6: The experiments presented in this figure have been recorded using different probes and MAS frequencies and according to the following systematic approach: the wet gel is analyzed in a 4 mm CRAMPS rotor at  $\nu_{\text{MAS}} = 12$  kHz and  $B_0 = 7.04$  T to maximize the amount of matter, where FSLG homonuclear decoupling scheme is employed in the corresponding HETCOR experiments. The dried gel was analyzed either in a 1.3 mm rotor spinning at  $\nu_{\text{MAS}} = 65$  kHz (no homonuclear decoupling schemes

applied) to reduce the strong homonuclear dipolar coupling or in 2.5 mm rotor spinning at  $\nu_{\text{MAS}} = 20$  kHz using DUMBO homonuclear decoupling scheme, both probes used at  $B_0 = 16.4$  T. The 2.5 mm probe nicely combines moderately high  $\nu_{\text{MAS}}$  and enough volume to run  $^{13}\text{C}$  CP MAS experiments in a reasonable amount of time (less than 1 hour) with respect to the 1.3 mm probe. The DUMBO sequence was optimized only for the 2.5 mm probe mounted on the  $B_0 = 16.4$  T spectrometer.

a) Series of  $^1\text{H}$  spectra recorded on dried C18:0 sophorolipid ribbons at different MAS frequencies, where the effect of the DUMBO homonuclear decoupling scheme at  $\nu_{\text{MAS}} = 20$  kHz is shown. Asterisks indicate artifacts due to DUMBO decoupling.<sup>8</sup> b)  $^{13}\text{C}$  CP MAS spectra recorded at contact time,  $t_c = 3$  ms, on a wet and dried gel of C18:0 sophorolipid ribbons. c) Typical HETeronuclear CORrelation (HETCOR) pulse scheme with implemented high-power homonuclear decoupling during  $t_1$  evolution for 2D implementation. Here, either FSLG or DUMBO homonuclear decoupling schemes have been employed.  $t_{90^\circ}$  is the  $90^\circ$  pulse on the  $^1\text{H}$  nucleus, CP is the Cross Polarization block with  $t_c$  being the contact time, while heteronuclear decoupling is applied on the  $^1\text{H}$  channel during signal acquisition on the  $^{13}\text{C}$  nucleus. d)  $^{13}\text{C}$ - $^1\text{H}$  HETCOR CP-MAS FSLG NMR experiment ( $t_c = 3$  ms) performed on the C18:0 sophorolipid ribbons (wet gel). e)  $^{13}\text{C}$ - $^1\text{H}$  HETCOR CP-MAS DUMBO NMR experiment ( $t_c = 3$  ms) performed on the C18:0 sophorolipid ribbons (dried gel).

Figure S6 presents a series of solid state NMR experiments recorded on C18:0 sophorolipid chiral fibers either in a wet gelly or dried form. The former was tested to keep hydration as a constant parameter, while the latter was performed to maximize the amount of condensed matter in the rotor, necessary to obtain high quality  $^{13}\text{C}$  CPMAS spectra. The  $^1\text{H}$  and  $^{13}\text{C}$  chemical shift attribution are listed in the table below.<sup>9</sup> One should note the fact that a downfield 3 ppm shift characterizes the resonances of the aliphatic chain and this is due their tight packing in an *all-trans* conformation.<sup>10</sup>

	Functional group	$^{13}\text{C}$ Chemical shift (ppm)	$^1\text{H}$ Chemical shift (ppm)
Aliphatic chain	C18 <sub>C</sub>	23.7	1.5
	C17 <sub>C</sub>	82.6	4.5
	(CH <sub>2</sub> ) <sub>x-C</sub>	33.1	1.5
	C3 <sub>C</sub>	28.2	1.5
	C2 <sub>C</sub>	38.5	1.9
	C1 <sub>c</sub>	175.0	5.6
Sophorose	C1 <sub>s</sub>	104.3	4.2
	C2,3,5 <sub>s</sub>	74.7	4.1
	C4 <sub>s</sub>	69.5	4.1
	C6 <sub>s</sub>	60.5	4.4

<sup>9</sup> M. Konishi, T. Fukuoka, T. Morita, T. Imura, D. Kitamoto, J. Oleo Sci., 2008, 57, 359-369

<sup>10</sup> A. Ulman, Adv. Mater. 1990, 2, 573

Figure S6a shows the typical spectrum of the dried gel at  $\nu_{\text{MAS}} = 20$  kHz and characterized by a lack of resolution; this is due to the strong  $^1\text{H}$ - $^1\text{H}$  homonuclear dipolar coupling occurring in the dried gel undoubtedly due to an extended network of hydrogen bonding. Resolution can be recovered either by employing very fast MAS ( $\nu_{\text{MAS}} = 65$  kHz) with a consequent reduction in the amount of matter (use of 1.3 mm rotor) or by employing complex high-power homonuclear decoupling pulse schemes, like the DUMBO sequence.<sup>7</sup> As shown in Figure S6a, use of DUMBO decoupling scheme at  $\nu_{\text{MAS}} = 20$  kHz allows to recover a  $^1\text{H}$  spectrum with an equivalent resolution obtained in a fast MAS experiment, even if artifacts are commonly generated.<sup>8</sup> Here, the experimental acquisition parameters were optimized so to reduce the amount and intensity of the artifacts.

Since we have run experiments on both dried and wet gels, we tested the effect of drying on  $^{13}\text{C}$  CP MAS spectra, shown in Figure S6b. Despite some minor variations in the relative intensity for peaks at about 104 ppm and 74 ppm, which are anyway impossible to quantify due to the fact that spectra are acquired under cross polarization conditions, the overall signal in both spectra is very similar. This suggests that drying does not have a crucial effect on the ribbon structure. Additionally, we have also verified that the ribbon structure is preserved after the drying process by mean of classical TEM (images not shown here), performed on the C18:0 sophorolipid chiral fibers coated with 0.8 nm Pt, necessary to protect the objects under the electron beam.

Demonstration of a symmetrical MLM configuration was done using  $^1\text{H}$ - $^{13}\text{C}$  2D HETCOR CPMAS experiments on both the wet and dried gels, and whose pulse program is shown in Figure S6c. In particular, we highlight the fact that homonuclear decoupling was applied during  $t_1$  evolution, thus reducing spin diffusion effects and recovering a high-resolution  $^1\text{H}$  dimension in the 2D correlation map.

The typical 2D heteronuclear correlation map between  $^{13}\text{C}$  and  $^1\text{H}$  for the wet gel of the C18:0 sophorolipid at pH= 6 is shown in Figure S6d. Cross-peaks enclosed in brackets A and B represent the through-bond correlation between  $^1\text{H}$  and  $^{13}\text{C}$  belonging to the same functional group, that is, respectively  $\text{CH}_2$  in the aliphatic chain and CH in sophorose. Interestingly, one can also observe cross-peaks D, E and F, which can be attributed to the through-space correlation between protons from sophorose (positions 1 to 6) and the aliphatic chain ( $\text{C}_{2\text{C}}$ ,  $\text{C}_{3\text{C}}$ ,  $(\text{CH}_2)_{\text{x-C}}$ ). Unfortunately, no exploitable COOH signal can be observed in a reasonable amount of time, most likely due to the low amount of matter in the rotor. These

observations support the idea that sophorose group is very close to the aliphatic chain, a fact that can only be justified by flip-flop, symmetrical, conformation of the sophorolipids in a head-to-tail arrangement. In the case of an antisymmetrical conformation, one should hardly see cross-peaks D, E, F, or at least their intensities would be very low.

Further proof is given in the  $^1\text{H}$ - $^{13}\text{C}$  2D HETCOR map recorded on the dried gel of C18:0 sophorolipid at pH= 6 (Figure S6e). First of all, this experiment allows to recover an exploitable COOH signal at  $\delta = 175.0$  ppm, which was not the case for the wet gel sample. Secondly, the dotted squares indicate a clear interaction between the COOH region and sophorose (square 1 and 2). Proximity between the aliphatic chain and the COOH is also detected (square 3). Interestingly, sophorose carbons  $\text{C}_{2,3,5}$  and  $\text{C}_4$  seem to be the closest to COOH (square 2), which does not seem to be the case for  $\text{C}_1$  and  $\text{C}_6$ , whose corresponding cross-peaks at  $\delta = 5.6$  ppm in the 2D HETCOR map display a sensibly lower signal. Once again, these data can only be explained by a symmetrical MLM conformation rather than an antisymmetrical one.